

Electronic Supplementary Information (ESI) for

**Converting H⁺ from Coordinated Water into H⁻ Enables Super Facile
Synthesis of LiBH₄**

Kang Chen^a, Liuzhang Ouyang^{a,*}, Hao Zhong^a, Jiangwen Liu^a, Hui Wang^a, Huaiyu
Shao^{b,*}, Yao Zhang^c, Min Zhu^{a,*}

*^a School of Materials Science and Engineering, Guangdong Provincial Key
Laboratory of Advanced Energy Storage Materials, South China University of
Technology, Guangzhou, China.*

*^b Joint Key Laboratory of the Ministry of Education, Institute of Applied Physics and
Materials Engineering (IAPME), University of Macau, Macau SAR, China.*

*^c School of Materials Science and Engineering, Jiangsu Key Laboratory of Advanced
Metallic Materials, Southeast University, Nanjing, China.*

*E-mail: meouyang@scut.edu.cn (L.Z. Ouyang)

*E-mail: memzhu@scut.edu.cn (M. Zhu)

*Email: hshao@um.edu.mo (H.Y. Shao)

List of Contents

1	Supporting Methods	3
2	Supporting Figures	7
3	Supporting Table	14
4	Supporting References	15

1 Supporting Methods

Purification and quantification of lithium borohydride. LiBH_4 was extracted by as-distilled diethyl ether from the ball-milling mixtures. It is worth noting that both MgO and remaining reactants are insoluble in diethyl ether. The extracted solution and undissolved side-products were separated by polytetrafluoroethylene membrane (0.45 μm). Afterward, the colatuie was transferred into a new glass bottle and evaporated under sliding vane rotary vacuum pump, while the solvent vapor (Et_2O) was captured by a cold trap placed in liquid nitrogen. Finally, the white solid powder (LiBH_4) was obtained through the aforementioned procedures. The amount of formed LiBH_4 was quantitatively determined by iodometric analysis¹⁻² and the LiBH_4 yield was calculated in accordance with the following equation:

$$\begin{aligned} \text{Yield} (\text{LiBH}_4) \\ = \frac{\text{obtained mass of LiBH}_4}{\text{theoretical mass of LiBH}_4} \times 100\% \end{aligned} \quad (1)$$

Notably, the LiBH_4 yield is referred to as a ratio of the mass of LiBH_4 actually converted by 1 mol of $\text{LiBO}_2 \cdot 2\text{H}_2\text{O}$ to the theoretical value. In addition, to test the accuracy of the quantitative method, 52.0mg of commercial LiBH_4 (95%), actually, 49.4mg of LiBH_4 was mixed into 100 mL of NaOH solution (0.25 mol/L). There was 48.7mg of LiBH_4 calculated by iodometric analysis. Then, the error of iodometric analysis was 1.4%, which was acceptable for quantification of LiBH_4 . Moreover, 50.1mg of commercial LiBH_4 (actually 47.6mg) was dissolved into 20 mL of as-distilled Et_2O and the extraction was evaporated via vacuum drying. There was 46.7mg of LiBH_4 quantified by iodometric analysis. The error calculation was also below 2%.

Ionic conductivity. Since the discovery of superior Li^+ conductivity in the HT (High temperature) phase, LiBH_4 has attracted much attention as solid-state electrolytes (SSEs) with high compatibility with Li electrode, negligible electronic conduction, and low grain boundary resistance³ compared to oxide-type or sulfide electrolyte systems⁴⁻⁵. However, LiBH_4 acts as an electrical insulator with LT (low-temperature) Li^+ conductivity $< 10^{-7} \text{ S cm}^{-1}$ ⁶, which falls short of the commercial demand ($> 10^{-3} \text{ S cm}^{-1}$). As expected, the structural deformation by inducing defects and changing the atomic arrangement⁷⁻⁸ could improve Li^+ conductivity of LiBH_4 . Especially, we succeeded in synthesizing $\text{LiBH}_4 \cdot \text{NH}_3$ from the regenerated LiBH_4 and the commercial one, respectively. Ionic conductivity of $\text{LiBH}_4 \cdot \text{NH}_3$ was obtained according to the following procedures.

The powder samples were loaded into a stainless-steel mould with a diameter of 13 mm and pressed into pellets as solid electrolyte with thickness of ~ 1 mm under a pressure of 20 MPa initially. Two metallic lithium foils of 13.5 mm diameter were then placed on the two sides of pellets to form test electrodes, and loaded in an airtight sample holder. All preparations took place in a glove box (Mikrouna, China) filled with Ar gas. Afterward, the ionic conductivity of pellets was measured by alternating current (AC) impedance spectroscopy in a frequency range from 1 Hz to 1 MHz with an electrochemical workstation (Gamry Interface 1000 and CHI604C, Chenghua, Shanghai). The airtight sample holder was placed in an oil bath and held for 30 min to control the temperature. Testing temperatures were ramped from room temperature (28 °C) to 45 °C. In addition, $\text{LiBH}_4 \cdot \text{NH}_3$ was prepared by exposing the as-purified LiBH_4

or commercial LiBH_4 to an atmosphere of high-purity ammonia (99.999%) with 1 bar pressure at room temperature for 2 h and evacuated by sliding vane rotary vacuum pump for 3 h⁹⁻¹⁰.

The XRD patterns of $\text{LiBH}_4 \cdot \text{NH}_3$ from as-purified product and commercial product are shown in **Fig. S6a**, which shows a good agreement with other's report⁸. The lithium-ionic conductivity was tested using two pieces of lithium foil electrodes in the typical Nyquist plots. **Fig. S7** shows partial of impedance plots of $\text{LiBH}_4 \cdot \text{NH}_3$ acquired from the as-purified LiBH_4 , as well as the commercial one at different temperatures. The resistance R concerned about ionic conductivity could be obtained from the intersection of a single arc or semi-circle with the Z' axis in the low-frequency limit from the Nyquist plots¹¹⁻¹². Therefore, the conductivity σ in accordance with following equation¹³⁻¹⁴:

$$\sigma = \frac{d}{AR} \quad (2)$$

wherein, σ , A, d, and R correspond to the conductivity, area of pellet, thickness and resistance of electrolytes, respectively. Nevertheless, LiBH_4 acts as an electrical insulator with LT Li^+ conductivity $< 10^{-7} \text{ S cm}^{-1}$, which is far from meeting the commercial demand ($> 10^{-3} \text{ S cm}^{-1}$). NH_3 was introduced to increase the defects and change the atomic arrangement of LiBH_4 -based crystal structure, for improving its LT Li^+ conductivity.

The Arrhenius plots of lithium borohydride mono-ammoniate ($\text{LiBH}_4 \cdot \text{NH}_3$) are shown in **Fig. S6b**, it is found that $\text{LiBH}_4 \cdot \text{NH}_3$ obtained from the as-purified LiBH_4

exhibits similar conductivity increasing with the ramping temperature as the commercial one and shows higher conductivity of up to $1.20 \times 10^{-3} \text{ S cm}^{-1}$ near room temperature (43 °C), higher than that of LiBH_4 ($10^{-7} \text{ S cm}^{-1}$) by 4 orders of magnitude^{6, 15}. It should be noted that a drastic increase in ionic conductivity occurs around 37 °C due to the structural change resulting from the formation of Schottky defects when ammonia is desorbed and it brings position vacancy⁸. This is the reason why the conductivity in cooling process is better than that in heating process.

2 Supporting Figures

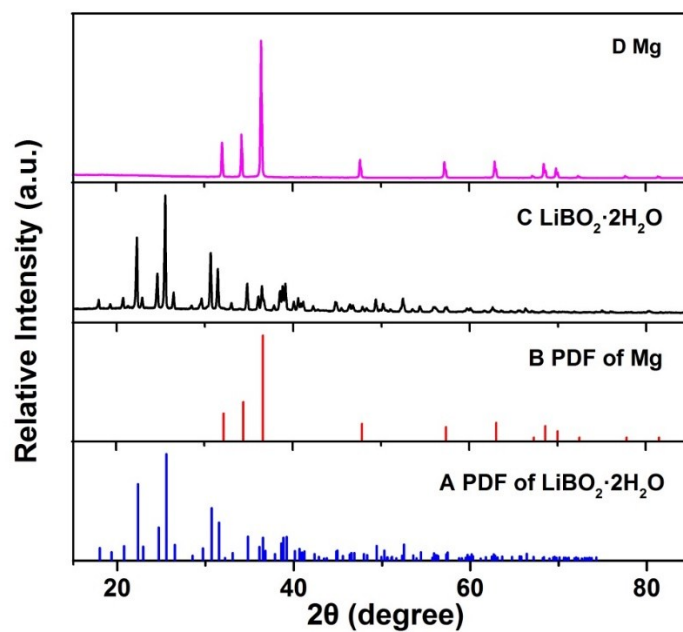


Fig. S1 XRD patterns of raw materials. (A) PDF card of $\text{LiBO}_2 \cdot 2\text{H}_2\text{O}$ (JCPDS 01-074-1509), (B) PDF card of Mg (JCPDS 00-035-08), (C) As-prepared $\text{LiBO}_2 \cdot 2\text{H}_2\text{O}$ from LiBO_2 aqueous solution, and (D) Pristine Mg.

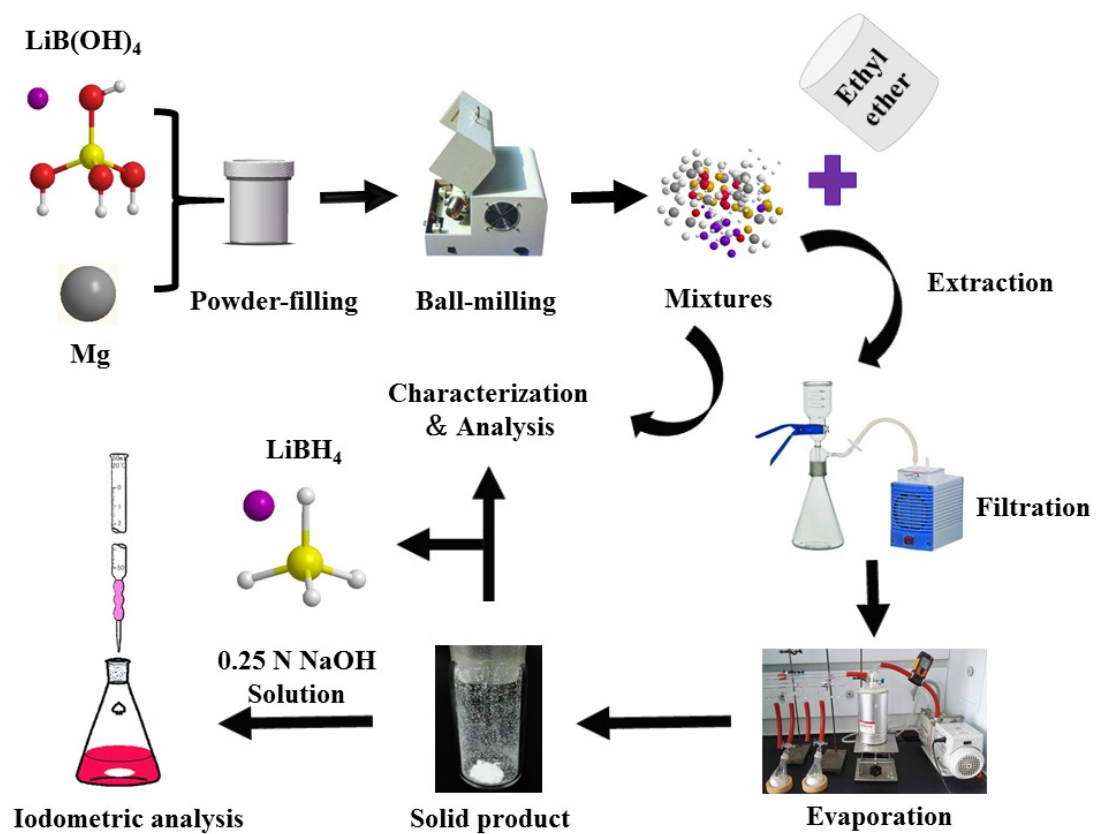


Fig. S2 Schematic flow of the experimental procedures.

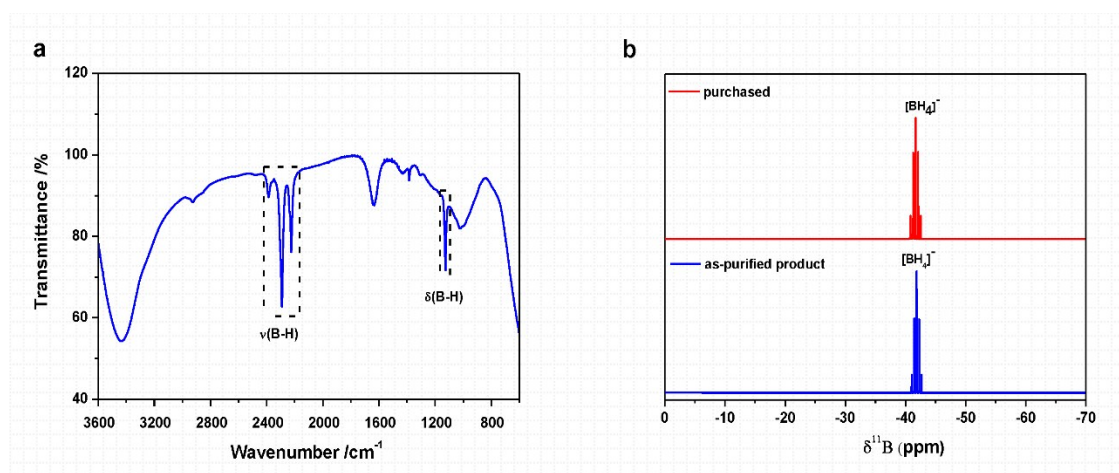


Fig. S3 FT-IR and NMR measurements. a, FT-IR spectrum of the product after ball-milling Mg and LiBO₂·2H₂O mixtures (in 5.0:1 mole ratio) for 15h. b, Solution-state (Tetrahydrofuran-d₈) ¹¹B (¹H coupled) NMR spectra of commercial LiBH₄ and purified product.

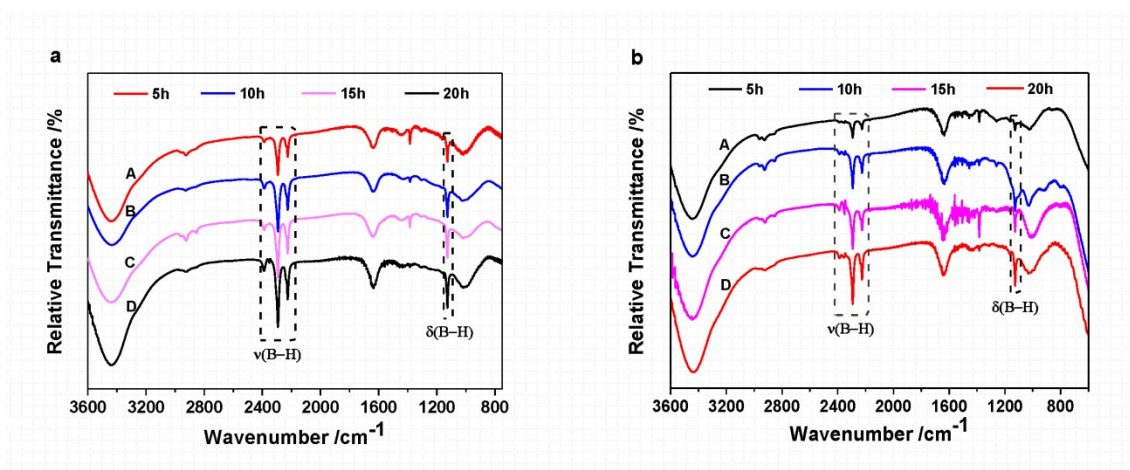


Fig. S4 FT-IR spectra. a, FT-IR spectroscopy of Mg and $\text{LiBO}_2 \cdot 2\text{H}_2\text{O}$ mixtures (in 5.0:1 mole ratio) after ball-milling for different durations: (A) 5h, (B) 10h, (C) 15h, and (D) 20h. b, FT-IR spectra of Mg and $\text{LiBO}_2 \cdot 2\text{H}_2\text{O}$ mixtures (in 5.5:1 mole ratio) under same condition: (A) 5h, (B) 10h, (C) 15h, and (D) 20h.

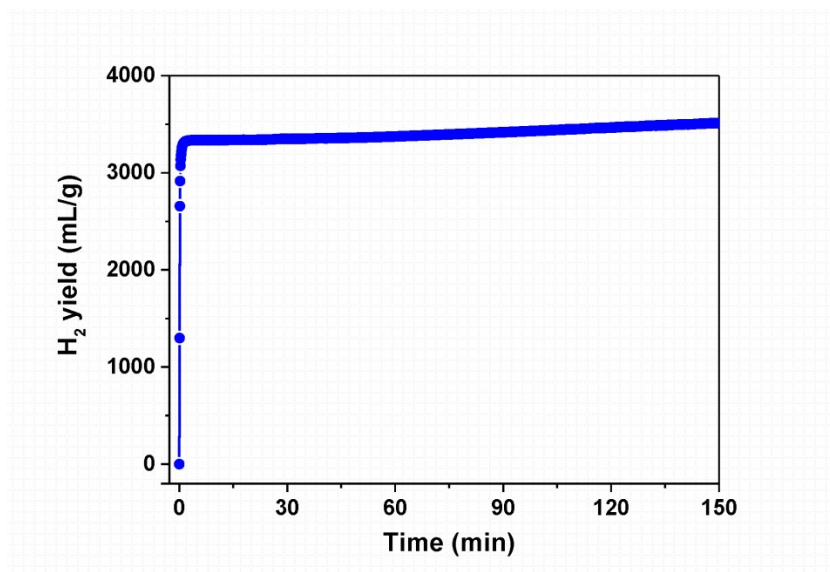


Fig. S5 Hydrolysis curve of the regenerated LiBH_4 in 2 wt.% CoCl_2 aqueous solution with a molar ratio of $\text{H}_2\text{O}/\text{LiBH}_4 = 4$. The hydrogen yield of the as-purified product is 3294 mL g^{-1} in 60s, then followed by a sluggish kinetics.

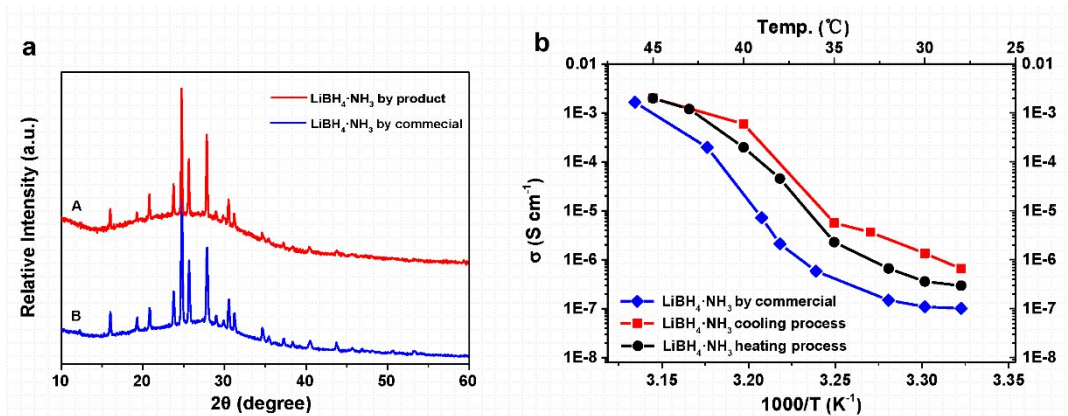


Fig. S6 Ionic conductivity tests. a, The XRD patterns of LiBH₄·NH₃ from (A) as-purified product and (B) commercial LiBH₄. b, Arrhenius plots of the ionic conductivities for LiBH₄·NH₃ obtained by as-purified LiBH₄ in heating process (black), cooling process (red), and LiBH₄·NH₃ by commercial product (blue) at different temperatures.

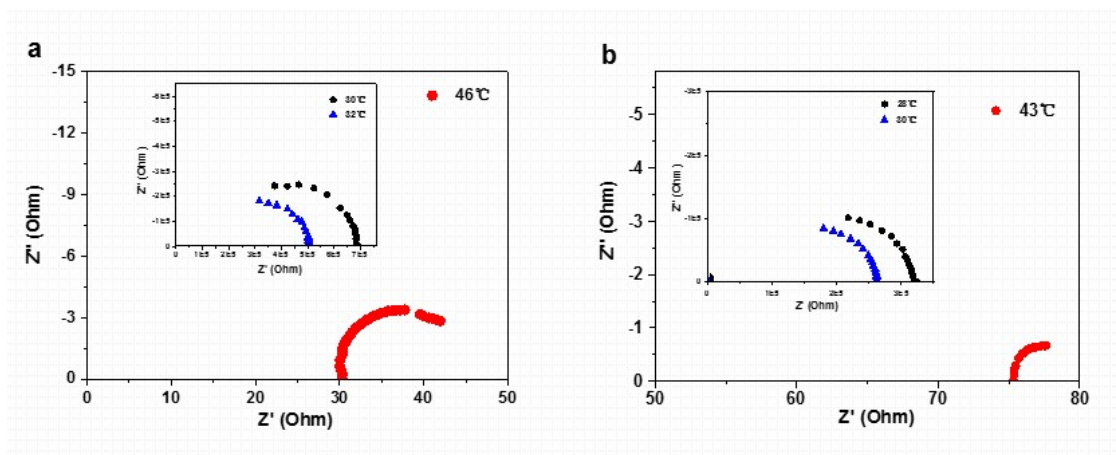


Fig. S7 Typical Nyquist plots of impedance data obtained using a lithium-metal electrode. a, $\text{LiBH}_4 \cdot \text{NH}_3$ from commercial LiBH_4 under different temperatures. b, $\text{LiBH}_4 \cdot \text{NH}_3$ from as-purified LiBH_4 in heating process under varied temperatures.

3 Supporting Table

Table S1. Material cost of LiBH₄ produced by ball milling Mg and LiBO₂·2H₂O and commercial method.

Method	Cost (US \$/ ton)
Ball milling Mg and LiBO ₂ ·2H ₂ O	34670 ^a
Commercial method	171818 ^b

^aThe calculation is based on the yield of 38.7% LiBH₄ when Mg and LiBO₂·2H₂O mixture with a ratio of 5.0:1 is ball milled for 20h. Then 14.41 tons of Mg are required to produce 1 ton LiBH₄. The price of Mg is \$2406/ton, which is available from China nonferrous metal network ^[16]. Then the total cost of raw materials is \$34670/ton.

^bThe price is from a commercial company in China. Commercial method refers to wet

chemical reaction method ^[17-18]: NaBH₄ + LiCl $\xrightarrow[75\%]{\textit{isopropylamine}}$ LiBH₄ + NaCl.

According to a yield of 75% in current industrial production, 2.59 tons of LiCl and 2.32 tons of NaBH₄ are needed for production of 1 ton LiBH₄. Then the total cost of raw materials is \$171818 due to the prices of LiCl and NaBH₄ being \$25769/ton and \$45291/ton, respectively ^[19].

4 Supporting References

1. Lyttle DA, Jensen EH, Struck WA. *Anal. Chem.* 1952, **24(11)**, 1843-1844.
2. C. L. Hsueh, C. H. Liu, B. H. Chen, C. Y. Chen, Y. C. Kuo, K. J. Hwang, J. R. Ku. *Int. J. Hydrogen Energy* 2009, **34(4)**, 1717-1725.
3. Y. Yan, R.-S. Kühnel, A. Remhof, L. Duchêne, E. C. Reyes, D. Rentsch, Z. Łodziana, C. Battaglia. *Adv. Energy Mater.* 2017, **7(19)**, 1700294.
4. K. Takada. *Acta Mater.* 2013, *61(3)*, 759-770.
5. F. Mizuno, A. Hayashi, K. Tadanaga, M. Tatsumisago. *Adv. Mater.* 2005, **17(7)**, 918-921.
6. M. Matsuo, S.-i. Orimo. *Adv. Energy Mater.* 2011, **1(2)**, 161-172.
7. M. Matsuo, A. Remhof, P. Martelli, R. Caputo, M. Ernst, Y. Miura, T. Sato, H. Oguchi, H. Maekawa, H. Takamura, A. Borgschulte, A. Züttel, S.-i. Orimo. *J. Am. Chem. Soc.* 2009, **131(45)**, 16389-16391.
8. T. Zhang, Y. Wang, T. Song, H. Miyaoka, K. Shinzato, H. Miyaoka, T. Ichikawa, S. Shi, X. Zhang, S. Isobe, N. Hashimoto, Y. Kojima. *Joule* 2018, **2(8)**, 1522-1533.
9. Y. H. Guo, W. W. Sun, Z. P. Guo, H. K. Liu, D. L. Sun, X. B. Yu. *J. Phys. Chem. C* 2010, **114(29)**, 12823-12827.
10. S. Li, W. Sun, Z. Tang, Y. Guo, X. Yu. *Int. J. Hydrogen Energy* 2012, **37(4)**, 3328-3337.
11. M. Xiang, Y. Zhang, L. Zhan, Y. Zhu, X. Guo, J. Chen, Z. Wang, L. Li. *J. Alloys Compd.* 2017, *729(30)*, 936-941.
12. Y. Zhang, L. Zhan, X. Zhuang, Y. Zhu, N. Wan, X. Guo, J. Chen, Z. Wang, L. Li. *J. Alloys Compd.* 2017, **695(25)**, 2894-2901.
13. D. Sveinbjörnsson, J. S. G. Myrdal, D. Blanchard, J. J. Bentzen, T. Hirata, M. B. Mogensen, P.

- Norby, S.-I. Orimo, T. Vegge. *J. Phys. Chem. C* 2013, **117(7)**, 3249-3257.
14. D. Blanchard, A. Nale, D. Sveinbjörnsson, T. M. Eggenhuisen, M. H. W. Verkuijlen, Suwarno, T. Vegge, A. P. M. Kentgens, P. E. de Jongh. *Adv. Funct. Mater.* 2015, **25(2)**, 184-192.
15. T. Ikeshoji, E. Tsuchida, T. Morishita, K. Ikeda, M. Matsuo, Y. Kawazoe, S.-i. Orimo. *Phys. Rev. B* 2011, **83(14)**, 144301.
16. The price of Mg is available from: <http://www.cnmn.com.cn/>.
17. H. C. Brown, M. C. Yong, S. Narasimhan. *Inorg. Chem.* 1981, **20**, 4454-4456.
18. H. I. Schlesinger, H. C. Brown, B. Abraham, A. C. Bond. *J. Am. Chem. Soc.* 1953, **75**, 186-190.
19. Jinjinle chemical Co. LTD. for the price of LiCl and NaBH₄. Available from: <https://show.guidechem.com/gaidexinjjl/>.